



DEFECTS IN CADMIUM ZINC TELLURIDE (CdZnTe) – A REVIEW

Kulkarni Gururaj Anand

S.D.M.C.E.T., Dharwad, Karnataka, India

ABSTRACT

CdTe and CdZnTe crystals are being intensively studied for their fundamental importance and the technological applications such as X – ray, γ -- ray detectors, electro-optic modulators and laser windows. $Cd_{0.96}Zn_{0.04}Te$ ternary crystals are ideal substrates for growing $Hg_{1-x}Cd_xTe$ epitaxial layers which find wide applications as infrared (IR) detectors. This is due to the high IR transmittance of $Cd_{0.96}Zn_{0.04}Te$ crystals and their chemical and crystallographic compatibility with $Hg_{1-x}Cd_xTe$ epilayers. High IR transmission requires chemically and electrically homogeneous crystals free from extraneous second phase particles. This objective is one of the most difficult thermodynamic and technological problems in the growth of CdTe and related alloys. Single crystals of CdTe have a low absorption coefficient, $\alpha = 0.0002 \text{ cm}^{-1}$, in the 0.85 – 30 μm region of the IR spectrum. Extrinsic factors affecting α are - impurities, free carriers and scattering by precipitates. Although vertical Bridgman method usually results in undoped crystals, CdTe and CdZnTe crystals exhibit p-type conductivity with a high carrier concentration and the presence of tellurium inclusions/precipitates due to retrograde solid solubility curve in the phase diagram. Although extensive efforts have been made in the area of purification of the CdZnTe crystals by using 7N pure starting materials, still impurity pick up during growth due to high temperature melt growth, affects α . In this context, this paper presents a review of the defects in CdZnTe crystals. These include Te precipitates, Cd vacancies, dislocations and impurities.

KEYWORDS: CdTe, CdZnTe, HgCdTe, Te precipitates, Dislocations, SIMS, FTIR, etc.

INTRODUCTION

The ternary II-VI compound cadmium zinc telluride ($Cd_{1-x}Zn_xTe$ or CZT) has been used as a substrate material for infrared applications for many years. Crystals of mercury cadmium telluride (HgCdTe or MCT) are used in infrared devices to detect, or sense, the thermal radiation from objects and produce visible signals or images. The effectiveness of MCT as an infrared detector depends on its orderly, crystalline structure. Manufacturers try to avoid defects in MCT crystals by solidifying the material under very controlled conditions. One method for controlling the growth of the crystal is to solidify MCT on top of another material that has a similarly ordered atomic structure. This base material is called a substrate. For $Hg_{1-y}Cd_yTe$, $Cd_{1-x}Zn_xTe$ is the "substrate of choice" among scientists and many commercial producers. CZT serves as a stabilizing influence as the MCT crystal layer forms because, during growth, the atoms between the active detector and substrate join together with a tight, interlocking match between the two lattices. This match between the two lattices reduces stress on the active detector as it grows. To achieve nominal lattice match between the materials and minimize defects due to misfit dislocation, 4.4% of zinc content is needed for $Hg_{1-y}Cd_yTe$ ($y=0.2$) and 4.1% for $y=0.3$ (Kennedy *et al.* 1988 [1]; Murphy 1986 [2]). This $Hg_{1-y}Cd_yTe / Cd_{1-x}Zn_xTe$ two-layered material can be placed in the device so that only the substrate is exposed to the air, with the $Hg_{1-y}Cd_yTe$ crystal sealed in an inert gas or a vacuum within the device. Because $Cd_{1-x}Zn_xTe$ is transparent to thermal radiation, it does not interfere with the transmission of

heat signals to the active detector. Cadmium zinc telluride substrates are also used as a base material for the development of focal plane arrays required for the guidance system of anti-tank missiles (e.g. Nag, a third-generation "fire and forget" anti-tank guided missile with a range of 4 to 6 kilometers, uses Imaging Infra-Red (IIR) guidance having both day and night capability).

During the last decade, $Cd_{1-x}Zn_xTe$ crystals with $0.05 < x < 0.4$ have received a growing interest in the field of room-temperature x-ray and gamma-ray detectors (Doty *et al.* 1992 [3], Butler *et al.* 1992 [4]). Gamma ray emissions can serve as a signature for cancer tumors, valuable mineral deposits and radioactive waste. But until recently, detecting the rays required bulky and ultra-expensive cryogenically cooled systems. CZT emits a tiny electronic signal when hit by gamma rays. CZT detectors are already standing guard over dismantled atomic weapons and cancer detection applications could be next.

The $Cd_{1-x}Zn_xTe$ has a direct energy gap for all alloy compositions and is tunable from 1.5 to 2.3 eV at room temperature, for $x=0$ and $x=1$ respectively (Olego *et al.* 1985 [5]; Oettinger *et al.* 1992 [6]). It possesses many of the physical properties required for detector operation, such as high atomic number (Z) for efficient radiation-atomic interactions, large enough band gap for high bulk resistivity required to maintain low noise associated with leakage current in the detector, a large cross-section for the photoelectric absorption of gamma-rays necessary for efficient conversion of the gamma-ray energy to electrical energy, high intrinsic mobility-lifetime ($\mu\tau$) product, and reduced electronic noise.

Use of CdTe Based Substrates for IR Applications

The CdTe family materials (in particular CdZnTe) remain the substrate of choice for epitaxial growth of HgCdTe for use in high performance IR detectors and focal plane arrays. This is the case despite advances in the use of alternate substrate technologies such as buffered GaAs and GaAs on Si; these technologies, to date, have not reproducibly demonstrated device performance comparable to arrays made in HgCdTe grown on CdZnTe and CdTe. The quality of CdTe family materials has improved significantly over the past several years and so the quality and reproducibility of IR detectors has improved along with them. It is clear, however, that CdTe family substrates still have a significant impact on HgCdTe devices and that further research is required to reduce the effect of substrates on these devices [7].

Issues with CdTe Based Substrates

Unlike silicon or gallium arsenide, it is very difficult to grow large size single crystals of CZT due to some of its inherent properties. It has the lowest thermal conductivity among all semiconductors that makes it difficult to obtain planar solid-liquid interface, which is desirable for single crystal growth. Due to its high ionicity and weak bonding, defects are easily incorporated during growth. Also, it is well established that both the structural defects and impurity contents of $Hg_{1-y}Cd_yTe$ epitaxial layers are strongly influenced by the quality of the substrates used in the epitaxial growth process. A substrate of poor structural quality will result in a poor substrate/epilayer interface from which defects will propagate in to the epilayer.

Basically our focal plane arrays (FPAs) are backside illuminated, with the device connected to underlying silicon multiplexer, using a matrix of indium bumps. Thus the substrate should have high IR transmission to pass the radiation on to the detector for collection. High IR transmission requires chemically and electrically homogeneous crystals free from extraneous second phase particles. This objective is one of the most technologically challenging problems due to thermodynamic limitations in the growth of CdTe and related alloys. The bulk CdZnTe crystals grown from melt suffer from the inherent disadvantage of accommodating tellurium precipitates because of high growth temperature and phase diagram limitations. These tellurium (Te) precipitates condense as cadmium vacancies and Te interstitials during the cooling process, which contribute to intrinsic point defects [8]. Though extensive efforts have been made in the area of purification of the CdZnTe crystals by using 6N pure starting materials, still the high temperature melt growth leads to impurity pick-up during the growth process [9]. This deviation in the stoichiometry, especially due to free carriers, impurities and second phase tellurium precipitates, play a major role in reducing the infrared transmission through the substrate material. Also they affect the device performance when used for detector applications [10]. In this context an effort has been made here to review the defects in CdZnTe crystals.

Synthesis and Growth

Tennant *et al.* [11] and Triboulet *et al.* [12] have recently reviewed the CdTe, CdZnTe materials as substrate for MCT epitaxial growth and compared them to the

alternatives based on GaAs, sapphire and Si. Problems with the growth of CdTe, CdZnTe included low thermal conductivity, difficulty in seeding due to the need for superheated melts, ease of twin formation, tilts and rotations in the lattice, stoichiometry control, Zn segregation and impurities. However, they both conclude that despite the progress made in the alternative substrate materials, lattice-matched substrates still produce MCT epitaxial layers which give the best device performance. Crystal growth and subsequent processing of CdTe, CdZnTe requires precise knowledge of the existence of solid and liquid phases with respect to pressure, temperature and composition. The temperature versus composition (T – x) diagram for the Cd -Te system is shown in **Figure 1**.

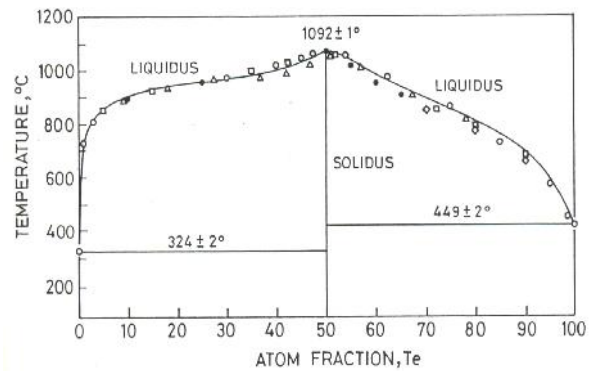


Figure 1: Temperature versus composition (T-x) diagram for the Cd-Te system [13].

The melting point, as seen from **Figure 1** is 1092 °C at approximately 50 atomic percent of Te and their individual melting temperatures are 324±2 °C and 449±2 °C on the Cd-rich and Te-rich sides of the phase diagram respectively.

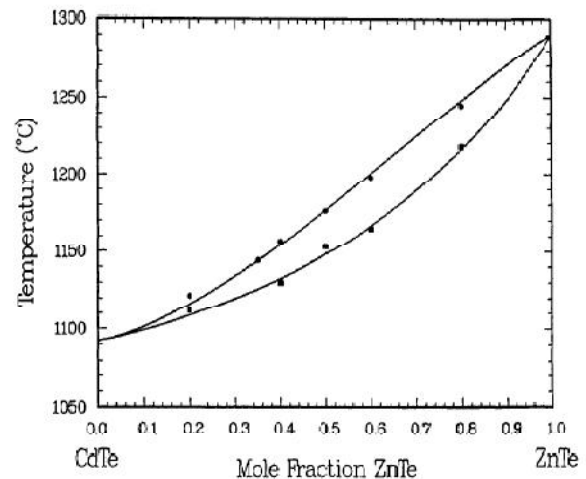


Figure 2: Pseudobinary section liquidus and solidus for the CdTe-ZnTe system [14].

Figure 2 shows the pseudobinary section liquidus and solidus curves for the CdTe – ZnTe system, where the data points are from the differential thermal analysis (DTA) measurements by Steininger *et al.* [14].

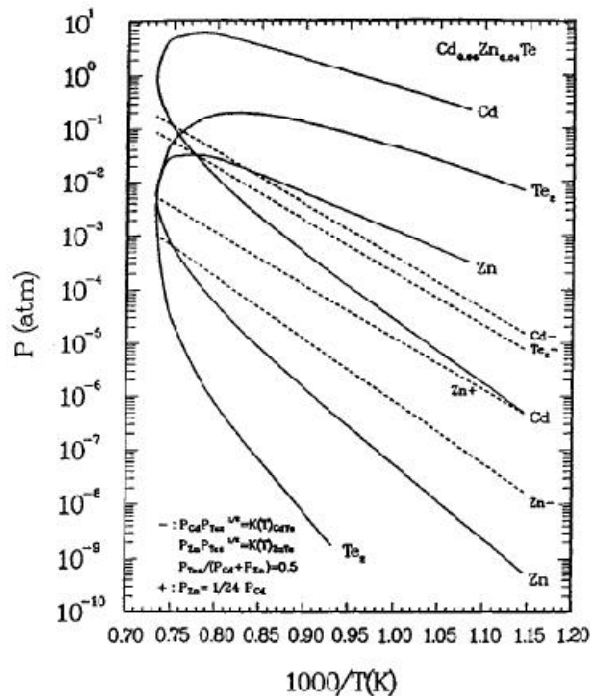


Figure 3: P_{Cd} , P_{Zn} , P_{Te_2} along 3-phase loops of $Cd_{0.96}Zn_{0.04}Te$ solid solution. Dashed lines satisfy equations in the lower left corner [15].

Figure 3 shows pseudobinary solid solution for $Cd_{0.96}Zn_{0.04}Te$. The three phase loops for P_{Cd} , P_{Zn} and P_{Te_2} (the partial pressures for Cd, Zn and Te_2 respectively) are shown as the labelled solid curves. The dashed lines labelled with an element name followed by a minus sign fall inside the three-phase curves. Therefore for each temperature in a wide range, there is a stable composition of $Cd_{0.96}Zn_{0.04}Te(s)$ for which the equilibrium vapor phase contains 50 at. % Te. Small deviations from 50 at. % Te in the solid are allowed. The existence of two Zn partial pressures, Zn^+ and Zn^- , illustrates that there is no congruently subliming composition.

Defects

(a) Segregation Coefficients

The segregation coefficients are mainly determined by mass spectrographic analysis or radiotracer profiles of the grown crystals. Knowledge of the values of these segregation coefficients is important for the growth of high purity CdTe and the zone-refining purification of CdTe boules [16]. The majority of the commonly encountered impurities have $k < 1$ (Li, Na, Al, Cl, K, Cu) while the others (Si, S, Zn, Se) have values close to 1.0. This leads to significant purification of the first-to-freeze regions of bulk crystals, though the contamination from the ampoule during growth can offset this.

Segregation of Zn

The segregation of Zn has a coefficient between 1.05 and 1.6 which causes significant yield losses in large crystals if uniformity of lattice matching is required. Radial segregation of Zn has also been observed and this has implications for both substrate yield and the understanding of the growth process. Segregation of Zn on the micro-scale has been determined in one study [17] and several

groups suggest supercooling occurs in the tip region of their crystals. The lowest segregation coefficient reported for Zn is 1.05, in a vertical Bridgman crystal grown with the Accelerated Crucible Rotation Technique [17].

Impurities

Impurity diffusion has been reported in the data review by P. Capper. These include diffusion of group I (H, Li, Cu, Au), II (Hg) and III (Ga, In), V (Sn, P, Bi), VI (O), VII (Cl, I) impurities and transition elements (Fe, Mn) in CdTe. Among these the most harmful is copper impurity. Harris *et al.* provided the evidence for copper out diffusion from CdTe leading to unintentional doping of MBE grown HgCdTe [18]. CdZnTe substrate copper contamination was found to degrade HgCdTe epitaxial layer and hence the performance of HgCdTe infrared (IR) detectors [19]. Gururaj Kulkarni has investigated for the passivation of the photoluminescence peak corresponding to the copper impurity observed in the photoluminescence spectra and predicted for the possible out diffusion of copper followed by in diffusion of zinc to replace copper by zinc and hence the formation of CdZnTe solid solution [20].

Iron is another impurity that is deleterious for the substrate applications of CdZnTe required for the growth and fabrication of HgCdTe IR detectors. According to mass spectroscopic data, Fe could occur in CdTe crystals as an unintentional impurity in concentrations of up to 10^{17} cm^{-3} [21]. Moreover, the solubility of iron at the melting point of CdTe is in excess of 10^{20} cm^{-3} [22]. The results of annealing experiments carried out on CdTe at $T > 800 \text{ }^\circ\text{C}$ have shown that this material could become contaminated with iron captured from insufficiently purified quartz [21]. Control of iron impurity in CdTe appears to be of great importance if the material is to be used as a substrate for the epitaxial growth of $Hg_{1-x}Cd_xTe$, since out diffusion of iron from the substrate into the epilayer deleteriously affects the performance of $Hg_{1-x}Cd_xTe$ infrared detectors [23]. On the contrary the incorporation of Fe can lead to interesting magnetic properties in semiconductors for spintronic applications [24].

Gururaj Kulkarni *et al.* have carried out secondary ion mass spectroscopy (SIMS) measurements on CdZnTe samples taken from different growth runs of the vertical Bridgman growth method and report on their typical mass spectra collected in the range of 0 – 150 amu to be depicting the presence of Li, Na, Al, Si, K, Ca, Fe, Ga, Ga_2 impurities along with the host matrix elements Cd, Zn and Te. They clearly report on the identification of Fe as one of the major impurities in some of the CdZnTe crystals and have further carried out a systematic study of the effect of Fe for its magnetic activity using low temperature ESR, SQUID and AC susceptibility measurements and for its optical activity using low temperature FTIR measurements. Signatures of Fe^{2+} and Fe^{3+} charge states of iron have been identified in undoped CdZnTe (Zn ~ 4 %) crystals grown in GE – 214 grade quartz crucibles. Fe^{2+} being optically active shows an absorption around 2295 cm^{-1} in the low temperature Fourier transform infrared (FTIR) spectra, while Fe^{3+} being magnetically active exhibits coexistence of para and ferromagnetic phases as identified by low temperature electron spin resonance (ESR) spectra and verified independently by low temperature superconducting

quantum interference device (SQUID) and AC susceptibility measurements [25].

Cd Vacancies

Cd vacancies are the point defects introduced into the CdTe matrix during the growth process due to retrograde solubility curve in the phase diagram.

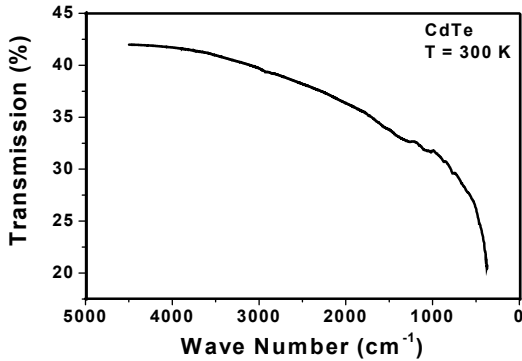


Figure 4: FTIR transmission spectra of CdTe

Figure 4 shows the FTIR transmission spectra of CdTe crystal. Here monotonic decrease in the transmission is to be seen with decreasing wave number. Such a behavior is due to the presence of Cd vacancies, thus indicating p-type behavior. The trend can be explained using the inter-valence band transition i.e. an electron in the light hole band can be excited to the heavy hole band by absorbing a photon. Cd vacancy point defects have been investigated using Photoluminescence as probe by Gururaj Kulkarni [26].

Dislocations

Dislocations are readily introduced into CdTe as a result of the relatively low hardness of this compound though a significant degree of strengthening is achieved by the addition of Zn. The microstructure is frequently subject to considerable local variations within a given crystal [27], and it is therefore desirable to assess both density and distribution of dislocations when characterizing these materials. The reduction of dislocation densities is of considerable importance in CdTe, CdZnTe owing to their applications as closely lattice matched substrates for CdHgTe epitaxial layers, it now being well recognized that the substrate dislocation density is one of the main factors limiting layer quality, while CdTe buffer layers are generally grown onto foreign substrates such as GaAs in order to limit the propagation of dislocations from the substrate/layer interface into active CdHgTe layers.

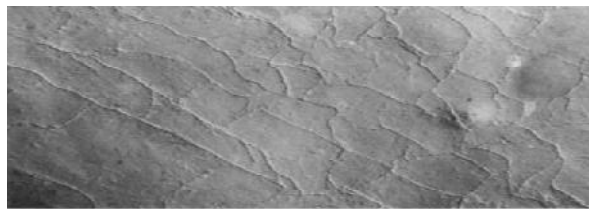
Dislocations in Bulk Crystals

Three types of dislocation distributions are generally found in CdTe bulk crystals grown by high temperature methods, e.g. Bridgman, gradient freeze or solvent evaporation. Firstly, deformation during post-growth cooling may occur. This effect may be marked by distinct slip bands, as revealed by etching and is associated with marked local strain birefringence when observed in the transmission IR microscope. Figure 5 shows slip lines, revealed by Br-methanol photo etching [28], in Bridgman CdTe grown in an uncoated silica ampoule.



Figure 5: Slip lines in Bridgman-grown CdTe [29]

Secondly, as a result of dislocation polygonisation, sub-grain boundary structure is formed throughout the material (Figure 6(a)). However, in the case of material grown in carbon coated ampoules the sub-grain boundaries are of a more diffuse appearance (Figure 6(b)).



(a)

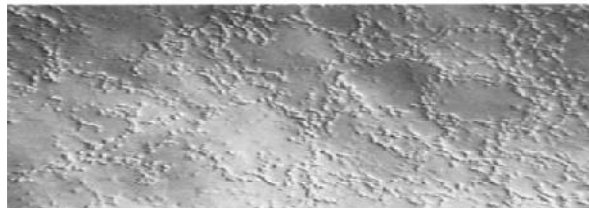


Figure 6: Sub-grain boundary structure in CdTe grown in (a) uncoated silica ampoule, (b) carbon coated ampoule (x 140) [29]

Thirdly, dislocations may occur at isolated intra-granular sites that are often randomly situated but may also be associated with precipitates, in which case clusters are produced, often in star-shaped patterns indicative of prismatic punching of extrinsic loops. However, the overall density of these dislocations is generally too low to allow accurate sampling in TEM specimens, and etch pitting or the CL or EBIC modes of the Scanning Electron Microscopy (SEM) are commonly used as means of indicating these defects. However, the effectiveness of these methods may be dependent on electrical or chemical effects associated with impurity decoration of the dislocations, while it may also be difficult to distinguish between dislocations or precipitates.

Precipitation

When non-stoichiometric CdTe, CdZnTe is cooled rapidly from high temperature, point defects concentrate owing to the retrograde solid solubility effect, leading to precipitation of second-phase material. Most work on precipitates in these materials has concerned second-phase Te, and a variety of techniques have been used to observe the defects, including etching [30-36], electron microscopy [30, 31, 35-41], transmission IR microscopy

[31, 32, 34, 36, 42], Auger electron spectroscopy [43, 44], Raman spectroscopy [45] and X-ray diffraction [43].

Te Precipitation

The sizes of Te precipitates reported in CdTe are very variable, with sizes ranging from 60 Å [39] to 100 μm [35]. This firstly reflects the wide range of growth and annealing conditions used to produce bulk crystals of this material. For example, the high post-solidification cooling rate experienced in many Bridgman systems is likely to result in a higher rate of precipitate nucleation than that of a solvent evaporation process [34]. Similarly, Nouruzi-Khorasani [40] showed that in CdTe annealed under Te-saturated conditions over the temperature range 460 – 900 °C, and then rapidly cooled, the size of intra-granular precipitates increased from 0.05 μm to 0.3 μm with increase in the annealing temperature. Secondly, however, the precipitation process is strongly influenced by the

availability of existing extended defects able to act as heterogeneous nucleation sites. Thus the largest Te precipitates are generally found on grain boundaries; **Figure 7** shows a scanning electron micrograph of a grain boundary precipitate, exposed by bromine-methanol polishing of Bridgman material grown from a Te-rich melt. **Figure 8** is a transmission electron micrograph of an intra-granular precipitate in the same material. Both these types of precipitates appear to be fully dense, with no associated void space, and neither, is there any evidence for locally high dislocation densities or marked strain birefringence (in the transmission IR microscope) associated with them. This suggests that the precipitation may involve both Te interstitials and Cd vacancies in a cooperative mechanism similar to that proposed for Cd_{0.2}Hg_{0.8}Te [45].

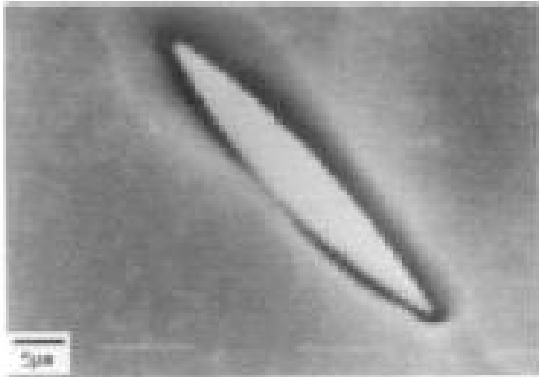


Figure 7: Grain boundary precipitate in CdTe, observed using scanning electron microscope

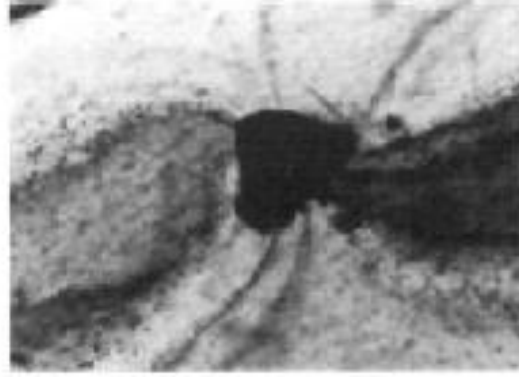


Figure 8: Intragranular precipitate in CdTe, observed using transmission electron microscope (x 1000) (x 12500)

Wada and Suzuki [32] showed using transmission IR microscopy that Te precipitates with dimensions of several microns or more exhibit well-defined faceting when viewed in <111> directions, and tend to change in shape from octahedral to tetrahedral as their size increases above 10 μm. Information on the structure of Te precipitates in Bridgman CdTe has been obtained by Shin *et al.* [43] using X-ray diffraction and Raman spectroscopy methods. It is found that the precipitates exist as the monoclinic, high pressure phase of elemental Te, this result being similar to that found for Te precipitates in CdHgTe [46]. It is noted that Te precipitates larger than about 10 μm may produce sufficient lattice strain to initiate prismatic punching of dislocation loops, as revealed by star-shaped patterns of etch pits [31-34]. For vapor-grown CdTe, Durose *et al.* [37] used transmission electron microscopy to identify radial strain contrast around small (~1 μm) intragranular precipitates. It is concluded by Gururaj Kulkarni *et al.* that, Te precipitates are the major unintentional and unwanted internal by products in the growth of CdZnTe crystals and play vital role in deciding its optical properties such as IR transmission, micro-Raman imaging

and NIR microscopy images. Using the micro-Raman maps and taking the spatial distribution of the area ratio of 121 to 141 cm⁻¹ Raman modes, the size and distribution of Te precipitates were estimated. The presence of Te precipitates under high pressure phase was detected by the blue shift of the Raman bands that appear at 121 (A₁) cm⁻¹ for a normal Te phase, indicating that these micro-Raman maps are basically the distribution of Te precipitates in different phases [47]. Yadava *et al.* [48] modelled the growth of Te precipitates in Te-saturated CdTe, assuming deviation from stoichiometry to be accommodated by Cd vacancies, Te antisites and Te interstitials. If it is assumed that the Te interstitial is the most abundant and/or mobile point defect species involved in the precipitation process, this model predicts that the growing, Te-rich liquid precipitates become pressurised, and that dislocation loop generation will occur in the matrix as the threshold pressure value is reached.

Changing composition by the addition of Zn to CdTe to achieve lattice matching with CdHgTe epilayer compositions also affects precipitation, as reported by Rai *et al.* [38]. Shahid *et al.* [36], claimed that Te precipitation

may be inhibited by the addition of Zn to CdTe. Capper *et al.* [42] used IR microscopy to reveal Te precipitation in both CdTe and $\text{Cd}_{0.96}\text{Zn}_{0.04}\text{Te}$, and made the further observation that a higher density of large (i.e. $>10\ \mu\text{m}$) precipitates was present in standard Bridgman crystals, compared with that of material grown by the accelerated crucible rotation technique (ACRT).

Removal of Precipitates

Removal of native precipitates from CdTe is most readily achieved by annealing in a saturated vapor of the element other than the precipitated species, i.e. Cd vapour to remove second-phase Te. However, this process leads to dislocation generation as a result of the need to accommodate extra volume as CdTe is produced by reaction between the Te precipitates and in-diffusing Cd interstitials. In addition, local optical and electrical effects are associated with the precipitate dissolution process, these being indicated by photochemical etching and IR transmission microscopy. Etching of CdTe in a 0.5% Br-methanol solution, without agitation, and exposed to strong white light, reveals dislocations and grain boundaries on all surface orientations [35]. It is generally found that these defects are marked by pits and grooves on n-type material, hillocks and ridges on p-type material, with the macroscopic etch rate of n-type material being greater than that of p-type material under illumination. Bridgman CdTe, p-type after growth under Te-saturated conditions, may be converted to n-type by Cd-saturated annealing. However, the electrical conversion process is locally retarded by the presence of Te precipitates, and this effect is clearly evident at Te decorated grain boundaries, which remain enclosed in a broad, p-type band despite the matrix having changed to n-type. **Figure 9** is an optical micrograph showing this in Bridgman CdTe, grown at $980\ ^\circ\text{C}$ from a Te-rich melt, and then annealed at $950\ ^\circ\text{C}$ under Cd-saturated conditions for 1 day.

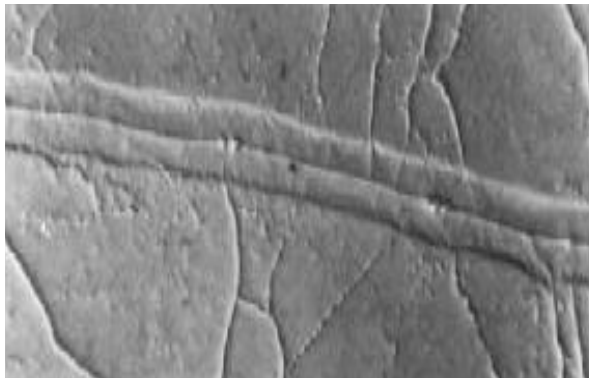


Figure 9 Te precipitate decorated grain boundary in CdTe annealed at $950\ ^\circ\text{C}$ under Cd-saturated conditions for 24 hrs (x 140) [49].

Near the surface of the same crystal, the reaction of intragranular Te precipitates with in-diffusing Cd is seen nearing completion (**Figure 10**); the remaining precipitates are at the center of raised, photo-etched discs, while the former sites of precipitates are marked by etch pits revealing the presence of clusters of dislocations generated by the removal process. These clusters are persistent and are associated with regions of strong optical

absorption, as shown in **Figure 11** which is a transmission IR micrograph of CdTe grown under Te-saturated conditions, and then annealed at $950\ ^\circ\text{C}$ for 5 days. These experiments have all been carried out under isothermal conditions [49].



Figure 10: Etch pit clusters revealing dislocations generated at sites of dissolving Te precipitates (x 140) [49].

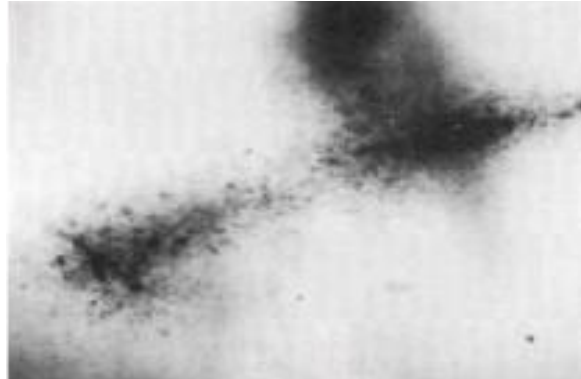


Figure 11: Regions of enhanced IR absorption at former sites of Te precipitates (x 240) [49].

Vydyanath *et al.* [50] carried out annealing of CdTe and $\text{Cd}_{0.96}\text{Zn}_{0.04}\text{Te}$ containing Te precipitates, over the temperature range $500 - 900\ ^\circ\text{C}$, using Cd/Zn pressures appropriate to stoichiometry, and postulated that the reported removal of large ($> 5\ \mu\text{m}$) Te precipitates could result from migration of the second-phase material under the action of temperature gradients if the Te melting point is exceeded during the anneal. However, it was noted that temperature gradient anneals are ineffective in removing small ($<1\ \mu\text{m}$) precipitates, probably because of the dominance of surface tension effects on this scale.

CONCLUSIONS

The study of defects in CdTe and CdZnTe is extremely complex and intriguing. The origin of many deep levels in both CdTe and CdZnTe still remain unclear. There has been a tremendous scatter on the energy level positions and possible identification of the intrinsic and extrinsic defects in CdTe and CdZnTe. Control of the second phase tellurium (Te) precipitates is a major challenge and is an urgent need, as it leads to the loss of useful signal in the $3 - 5\ \mu\text{m}$ atmospheric window. There are no direct

experimental ways for quantifying the Te precipitates without destroying the materials. Control of impurities is another challenge and an important requirement, if CdZnTe is to be used as a substrate material for the growth and fabrication of HgCdTe IR detectors. Especially the control of copper and iron impurities is of prime importance as they lead to the loss of useful signal in the mid-IR region and also their propagation into the HgCdTe epilayer affects the subsequent device performance. In this context, an effort has been made here to review some of these defects that are commonly observed in CdZnTe crystals, from the literature and author's own work.

BIBLIOGRAPHY

- [1] J.J. Kennedy, P.M. Amirtharaj, P. R. Boyd, S. B. Qadri, R. C. Dobbyn and G. G. Long, *J. Cryst. Growth* **86**, 93 (1988).
- [2] J. D. Murphy, *SPIE* **2**, 659 (1986).
- [3] F. P. Doty, F. Butler, J. F. Schetzina, and K. A. Bowers, *J. Vac. Sci. Technol.* **B10**,1418 (1992).
- [4] J.F. Butler, C.L. Lingren and F.P. Doty, *IEEE Transactions on Nuclear Science* **39**, 605 (1992).
- [5] D.J. Olego, J. P. Faurie, S.Sivanathan and P. M. Raccah, *Appl. Phys. Lett.* **47**, 1172 (1985).
- [6] K. Oettinger, D. M. Hofmann, A. L. Efros, B. K. Meyer, M. Salk and K. W. Bentz, *J. Appl. Phys.* **71**, 4523 (1992).
- [7] *Properties of Narrow Gap Cadmium based Compounds*, edited by P. Capper (INSPEC, IEE, London, UK, 1994) pp.601.
- [8] S. Sitharaman, R. Raman, L. Durai, S. Pal, M. Gautam, A. Nagpal, S. Kumar, S. N. Chatterjee and S. C. Gupta, *J. Cryst. Growth* **285**, 318 (2005).
- [9] A. K. Garg, M. Srivastava, R. C. Narula, R. K. Bagai and V. Kumar, *J. Cryst. Growth* **260**, 148 (2004).
- [10] S. Sen, D. R. Rhiger, C. R. Curtis, M. H. Kalisher, H. L. Hettich and M. C. Currie, *J. Electron. Mater.* **30**, 611 (2001).
- [11] W.E. Tennant, C.A. Cockrum, J.B. Gilpin, M.A. Kinch, M.B. Reine and R.P. Ruth, *J. Vac. Sci. Technol. B(USA)* **10**, 1359(1992).
- [12] R. Triboulet, A. Tromson-Carli, D. Lorans and T. N'Guyen Duy, *J. Electron. Mater. (USA)* **22**, 827 (1993).
- [13] D. de Nobel, *Philips Res. Reports (Netherlands)* **14**, 361 (1959).
- [14] J. Steininger, A.J. Strauss and R.F. Brebrick, *J. Electrochem. Soc. (USA)* **117**, 1305 (1970).
- [15] *Properties of Narrow Gap Cadmium based Compounds*, edited by P. Capper (INSPEC, IEE, London, UK, 1994) pp. 417 and the references therein.
- [16] D. de Nobel [*Philips Res. Rep. (Netherlands)*] **14**, (1959) pp.361-99 and pp.430-92].
- [17] *Properties of Narrow Gap Cadmium based Compounds*, edited by P. Capper (INSPEC, IEE, London, UK, 1994) pp.501-503 and the references therein.
- [18] K.A. Harris, R.W. Yanka, L.M. Mohnkern, A.R. Reisinger, T.H. Myers, Z.Yang, Z. Yu, S. Hwang and J.F. Schetzina, *J. Vac. Sci. Technol. B* **10**, 1574 (1992).
- [19] J.P. Tower, S.P. Tobin, M. Kestigian, P.W. Norton, A.B. Bollong, H.F. Schaake and C.K. Ard, *J. Electron. Mater.* **24(5)**, 497 (1995).
- [20] G. A. Kulkarni, K.S.R.K Rao and R.K.Sharma, *Proc. of the XIII International Workshop on Physics of Semiconductor Devices*, December 13 – 17, 2005,
- [21] B.M.Vul, V.S.Ivanov, V.A. Rukavishnikov, V.M.Sal'man and V.A.Chapnin, *Soviet Physics Semiconductors* **6(7)**, 1106 (1973).
- [22] G.A. Slack and S. Galginaitis, *Phys. Rev.* **133**, A253 (1964).
- [23] P. Capper, *J. Cryst. Growth* **57**, 280 (1982).
- [24] S.A. Wolf, D.D. Awschalom, R.A. Buhrman, J.M. Daughton, S. von Molnar, M.L. Roukes, A.Y. Chitchekanova and D.M. Treger, *Science* **294**, 1488 (2001).
- [25] G. A. Kulkarni, O.V.S.N. Murthy, K.S.R.K.Rao, S. V. Bhat and B.R. Chakraborty, *Solid State communications*, **150**, pp. 2174 – 2177 (2010).
- [26] G. A. Kulkarni, K.S.R.K Rao, A.K.Garg, M. Srivastava, R.Raman and F. Joseph Kumar, *International Symposium for Research Scholars on Metallurgy, Materials Science and Engineering*, December 18 – 20, 2006, IIT Madras, India. ID: AMO-O-04.
- [27] I. Hahnert and M. Wienecke, *Mater. Sci. Eng. B* **16**, 168 (1993).
- [28] D.J. Williams and A.W. Vere, *J. Cryst. Growth* **83**, 341 (1987).
- [29] *Properties of Narrow Gap Cadmium based Compounds*, edited by P. Capper (INSPEC, IEE, London, UK, 1994) pp.505-509 and the references therein.

- [30] K. Durose and G.J. Russell, *J. Cryst. Growth* **86**, 471 (1988).
- [31] C.C.R. Watson, K. Durose, A.J. Banister, E. O'Keefe and S.K. Bains, *Mater. Sci. Eng. B* **16**, 113 (1993).
- [32] M. Wada and J.Suzuki, *Jpn. J. Appl. Phys.* **27**, L972 (1988).
- [33] R.K. Bagai, G.L. Seth and W.N. Borle, *J. Cryst. Growth* **91**, 605 (1988).
- [34] A.W. Vere, V. Steward, C.A. Jones, D.J. Williams and N. Shaw, *J. Cryst. Growth* **72**, 97 (1985).
- [35] D.J. Williams [PhD Thesis, University of Birmingham, UK (1986)].
- [36] M.A. Shahid, S.C. McDevitt, S. Mahajan and C.J. Johnson [*Inst. Phys. Conf. Ser. (UK) no. 87 (1987) pp.321-5*].
- [37] K. Durose, G.J. Russell and J. Woods, *J. Cryst. Growth* **72**, 85 (1985).
- [38] R.S. Rai, S. Mahajan, S. McDevitt and C.J. Johnson, *J. Vac. Sci. Technol. B* **9**, 1892 (1991).
- [39] T.J. Magee, J. Peng and J. Bean, *Phys. Status Solidi A* **27**, 557 (1975).
- [40] A. Nouruzi-Khorasani [PhD Thesis, University of Birmingham, UK (1981)].
- [41] F.A. Selim, V. Swaminathan and F.A. Froger, *Phys. Status Solidi A* **29**, 465 (1975).
- [42] P. Capper, J.E. Harris, E.O'Keefe, C.L. Jones, C.K. Ard, P. Mackett and D.Dutton, *Mater. Sci. Eng. B* **16**, 29 (1993).
- [43] S.H. Shin, J. Bajaj, L.A. Moudy and D.T. Cheung, *Appl. Phys. Lett.* **43**, 68 (1983).
- [44] K. Yokata, T. Yoshikawa, S. Katayama, S. Ishihara and I. Kimura, *Jpn. J. Appl. Phys.* **24**, 1672 (1985).
- [45] D.J. Williams and A.W. Vere, *J. Vac. Sci. Technol. A* **4**, 2184 (1986).
- [46] H.F. Schaake and J.H. Tregilgas, *J. Electron. Mater.* **12**, 931 (1983).
- [47] G. A. Kulkarni, V.G. Sathe, K.S.R.K. Rao, D.V.S. Muthu and R.K. Sharma, *J. Appl. Phys.*, American Institute of Physics, **105**, 063512 (2009).
- [48] R.D.S. Yadava, R.K. Bagai and W.N. Borle, *J. Electron. Mater.* **21**, 1001 (1992).
- [49] *Properties of Narrow Gap Cadmium based Compounds*, edited by P. Capper (INSPEC, IEE, London, UK, 1994) and the references therein.
- [50] H.R. Vydyanath, J. Ellsworth, J.J. Kennedy, B. Dean, C.J. Johnson, G.T. Neugebauer J. Sepich and P.K. Liao, *J. Vac. Sci. Technol. B* **10**, 1476 (1992).